

Comparative Studies of Young Open Clusters

III. Empirical Isochronous Curves and the Zero Age Main Sequence

J. C. Mermilliod

Institut d'Astronomie, CH-1290 Chavannes des Bois, Suisse

Received January 14, accepted January 20, 1981

Summary. Empirical isochronous curves for open clusters younger than the Hyades have been determined from pairs of colour-magnitude diagrams for 14 age groups formed by Mermilliod (1980a). These curves have been drawn in a synthetic composite diagram which presents the observational results on stellar evolution in the M_V vs $(B-V)_0$ plane, based on 75 young open clusters. The ZAMS has been re-examined, as well as the $(U-B)_0$ vs $(B-V)_0$ relation, and the present results do not favour the ZAMS revision proposed by Eggen (1976). Absolute ages for each age group have been obtained from an age calibration based on a new grid of evolutionary models by Maeder (Maeder and Mermilliod, 1981).

A fine picture of stellar evolution has been traced out, especially concerning the red giants phase. It is found that a marked concentration of red giants, analogous to the clump in older open clusters, still exists for clusters as young as 2×10^8 y, with turn-up at B9. The mean $(B-V)_0$ colour indices of the concentrations remain near $(B-V)_0 = +1.0$, while the absolute magnitude becomes brighter. For younger clusters, the concentration is less marked and its mean colours become redder and redder while its mean absolute magnitude decreases. A linear relation has been established between the mean absolute magnitude of the red giant concentrations and $\log t$ in the interval: $7.3 < \log t < 8.9$. Extremely few stars are found in the middle of the Hertzsprung gap. This fact imposes strong constraints on the models describing loops in the HR diagrams.

Key words: open clusters - HR diagram - stellar evolution

1. Introduction

The amount of observational data presently available (Mermilliod 1976, 1980) makes it possible to study young open clusters in rather fine detail, and especially stellar evolution from an observational point of view. Even though the general characteristics of stellar evolution are well known, many points remain uncertain and, moreover, these ideas rely heavily on the HR diagrams of old or globular clusters. But information on the evolution of stars with large masses should be obtained from the analysis of the HR diagrams of young open clusters, although they generally contain few bright and massive stars. (This remark does not apply to several clusters, such as NGC 884 (χ Per), 2099, 6067, 6705). To overcome this difficulty, the composite diagram method has become necessary. Such diagrams have already been constructed by Barbaro et al. (1968) and more recently by Harris

(1976). But the too great age interval per group used in those papers prevented making the best of this method. Mermilliod (1980a) has worked out finer age subdivisions and formed 14 age groups, covering the age interval from NGC 6231 (turn-up at O9) and the Hyades (turn-up at A2), containing 4 to 8 open clusters each. New composite HR diagrams have been produced (Mermilliod, 1980a) by combining the diagrams of each cluster. The adopted procedure ensures that good age homogeneity exists in each group. This material has served as a basis for the determination of mean main sequences and the ZAMS, and for a discussion of stellar evolution.

In the following, section 2 presents the empirical isochronous curves, section 3 the $(U-B)_0$ vs $(B-V)_0$ relation, section 4 the new ZAMS, section 5 an absolute age calibration and section 6 a discussion.

2. Empirical Isochronous Curves

The estimation of the position and shape of the mean main sequence in the colour-magnitude diagram of any young open cluster is a real problem, which can be solved only approximately when dealing with a single open cluster. The present approach by means of composite diagrams opens new possibilities to free oneself of the main difficulty, i.e. the small number of member stars in many young open clusters.

The 12 pairs of composite diagrams established by Mermilliod (1980a) have been used to determine a homogeneous set of empirical isochronous curves for all age groups. The curves have been drawn by hand throughout the most populated sequence which is thought to be the "single stars" locus, allowing for some scatter because of observational errors. Thus they do not really form a lower envelope, but rather a mean line.

Careful attention has been paid to ensure internal coherence between all pairs of isochronous curves. This means that, at any value of M_V , the corresponding $(B-V)_0$ and $(U-B)_0$ indices form a single relation, which must be the same for all age groups and correspond to an observed composite diagram built from clusters showing the less scattered $U-B$ vs $B-V$ diagrams. The above condition is the only one that can be imposed to the determination of the empirical isochronous curves, owing to the properties of the UBV photometric system. The curves have been drawn in a synthetic composite diagram on the same sequence (Figs. 1 and 2).

Fig. 1 synthesizes the observational results on stellar evolution in the M_V vs $(B-V)_0$ plane as featured by the young open clusters, collecting information from

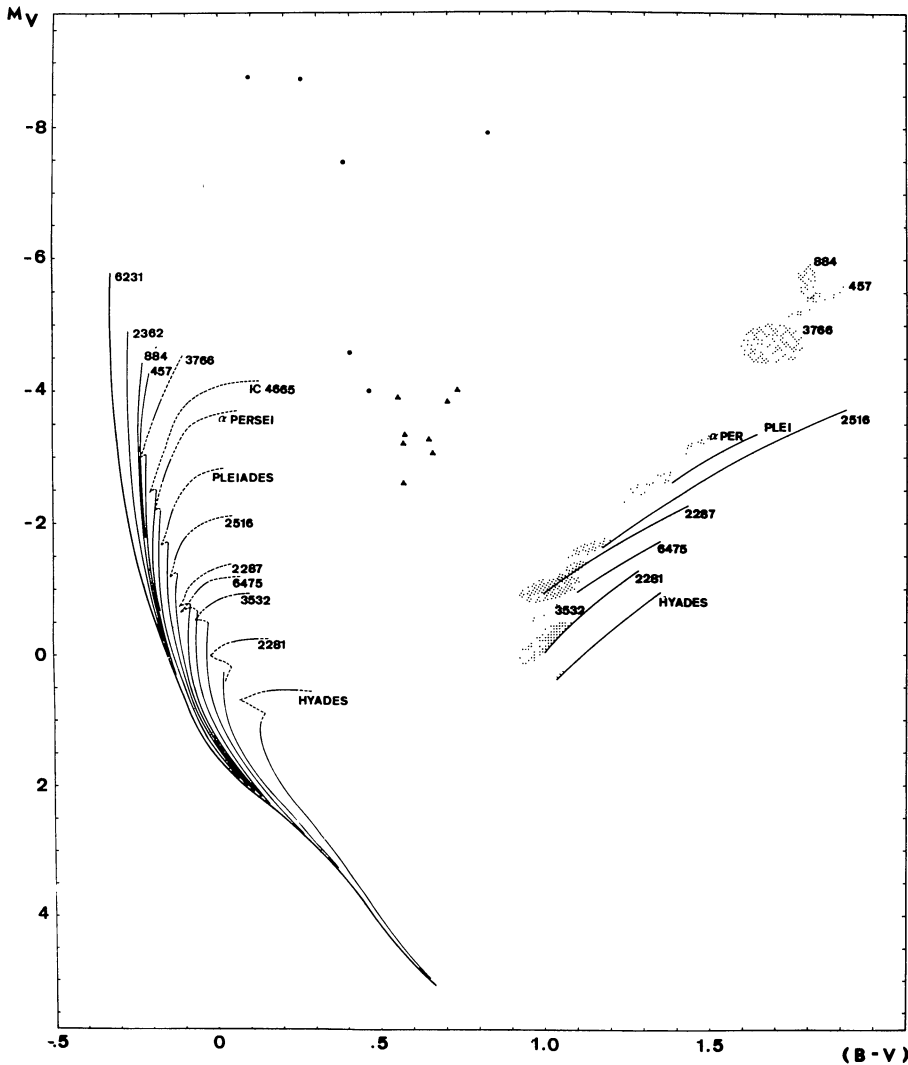


Fig. 1. Composite HR diagram presenting the sequences deduced from 14 pairs of composite diagrams (Mermilliod, 1980a). The age groups are designated by the name of the most representative cluster. The darkened areas show the positions of the red giant concentrations. Triangles stand for Cepheids and dots for non-Cepheid stars in the Hertzsprung gap. The dashed lines have been adapted from models by Maeder.

75 clusters. The image is thus far more refined than those presented previously (Sandage, 1957; Harris, 1976). Each age group is designated by the name of the most representative cluster, as adopted by Mermilliod (1980a). The upper part of the main sequence, corresponding to the overall contraction and shell-ignition phases, is practically impossible to describe empirically because of the rapidity of evolution leading to very few observable stars in this zone. Results from theoretical calculations by Maeder (Maeder and Mermilliod, 1981) have been superimposed and shown by dashed lines. The observed loci of the red evolved stars have also been drawn schematically. The darkened areas represent the position of the concentrations of red giants and supergiants. In the middle of the Hertzsprung gap, triangles have been placed for individual Cepheid variables (Table 1). The absolute magnitude and intrinsic colours have been taken from Sandage and Tammann (1969) for most stars and from Turner (1978) for CV Mon. Dots represent non-Cepheid stars in the Hertzsprung gap (Table 2).

The M_V vs $(U-B)_0$ plane (Fig. 2) has been limited to the main sequence because the data for the red giants are fewer in number and lower in quality. One notices immediately that the bluest $(U-B)_0$ colour index at the turn-up is a far better age indicator than $(B-V)_0$ in the

Table 1. List of Cepheids plotted in Fig. 1

Var name	Cluster	M_V	$(B-V)_0$
S Nor	NGC 6087	-4.03	0.73
DL Cas	NGC 129	-3.84	0.70
U Sgr	IC 4725	-3.93	0.55
CV Mon	Anon	-3.35	0.63
CE Cas a	NGC 7790	-3.27	0.64
CF Cas	NGC 7790	-3.07	0.65
CE Cas b	NGC 7790	-3.20	0.56
EV Sct	NGC 6664	-2.62	0.57

Table 2. List of non-Cepheid stars in the middle of the Hertzsprung gap, plotted in Fig. 1

Cluster - Star	HD	Sp.T.	M_V	$(B-V)_0$
IC 2581 - 1	90772	A5Ia	-8.78	0.09
NGC 457 - 136	7927	F0Ia	-8.75	0.25
NGC 2439 - 1	62058	G0Ia	-7.95	0.82
NGC 654 - 1	10494	F5Ia	-7.48	0.38
Me1 20 - 605	20902	F5Ib	-4.60	0.40
NGC 129 - 170	236438	F5Ib	-4.02	0.46

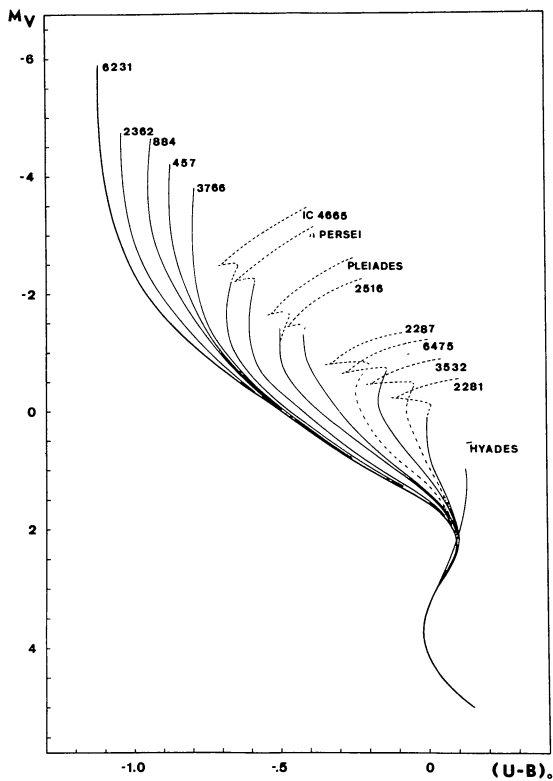


Fig. 2. Composite diagram presenting the empirical isochronous curves. The dot-dashed lines for the NGC 3532 and 2287 age groups have been obtained from the M_V vs $(B-V)_0$ sequence and the $(U-B)_0$ vs $(B-V)_0$ relation, because no M_V vs $(U-B)_0$ diagrams could be drawn for these two groups.

present age interval under consideration, i.e. open clusters younger than the Hyades. It is evident from the shape of the sequences in Fig. 2 that this particular plane loses almost all its usefulness for older clusters - thus the adopted age limit in this discussion.

Normal points of the empirical isochronous curves are given separately for the M_V vs $(B-V)_0$ plane (Table 3) and for the M_V vs $(U-B)_0$ plane (Table 4). They correspond to the evolved part of the curves, the ZAMS being excluded.

3. The $(U-B)_0$ vs $(B-V)_0$ Relation

The $(U-B)_0$ vs $(B-V)_0$ relation resulting from the processes described in the preceding section is presented in Fig. 3 and listed in Table 5. The condition of internal coherence applied to the determination of the isochronous curves is valid insofar as it has been shown, by Gutierrez-Moreno (1979) among others, that in the UBV plane there are no luminosity effects between the classes V to III, down to spectral type A0. This range of luminosity classes corresponds to the main sequence phase as a whole.

The slope of the sequence in the domain $(U-B)_0 < 0$ is different from the slopes of the sequences published by Golay (1974), Gutierrez-Moreno (1975) and Deutschman et al. (1976). On the other hand, the present sequence is nearly identical to that obtained by Heintze (1973)

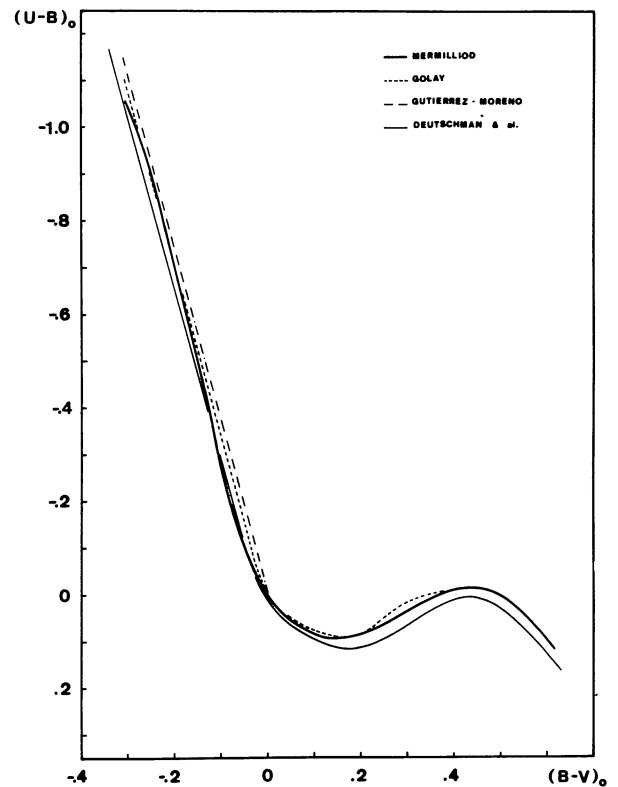


Fig. 3. Comparison of the present colour-colour relation with previous ones. In the $(U-B)_0 < 0$ domain this sequence is in very good agreement with Heintze's (1973).

through a different method. This very good agreement is gratifying.

In the interval $0.10 < (B-V)_0 < 0.40$ the estimation of the position of the sequence is critical. It depends on the reddening correction of the clusters, but above all, the estimation is rendered difficult by the gap in the distribution of the stars appearing in this domain (Böhm-Vitense and Canterna, 1974) resulting from the onset of convection in the stellar atmospheres. Consequently, the dot density is remarkably lower in this part of the sequence.

Moreover, one has also to take into account differential effects due to binarity, metallicity (either chemical composition or Am phenomenon), or evolution among the late A- and F-type stars. The latter are already perceptible at the Hyades age. All these facts contribute to the scatter in the observed sequences and make determination of the exact position of the colour-colour relation more uncertain. Deutschman et al.'s (1976) relation is strongly inspired by Eggen's and corresponds at best with the Hyades sequence which, as said before, is slightly evolved. The present sequence is closer to the Pleiades and α Persei observed diagrams.

4. Determination of the ZAMS

The present material may be used to redetermine the ZAMS, taken by definition as the extreme left envelope of the isochronous curves. The followed procedure is justified because no ZAMS, or any sequence given *a priori*, has

Table 3. Normal points in the M_V vs $(B-V)_0$ isochronous curves

M_V	6231	2362	884	457	3766	1C4665	α Per	Plei	2516	2287	6475	3532	2281	Hyades
-4.50	-.32	-.27												
-4.25	-.32	-.27												
-4.00	-.32	-.27	-.24											
-3.75	-.315	-.27	-.24	-.23										
-3.50	-.31	-.27	-.24	-.23										
-3.25	-.305	-.265	-.24	-.23										
-3.00	-.30	-.265	-.235	-.225	-.215									
-2.75	-.29	-.265	-.23	-.225	-.215		-.16							
-2.50	-.285	-.26	-.23	-.225	-.215		-.17							
-2.25	-.28	-.255	-.225	-.22	-.215	-.185	-.175							
-2.00	-.27	-.245	-.225	-.22	-.215	-.19	-.175							
-1.75	-.26	-.235	-.22	-.215	-.21	-.195	-.175							
-1.50	-.245	-.225	-.215	-.21	-.205	-.195	-.175	-.15	-.13					
-1.25	-.235	-.215	-.205	-.20	-.20	-.19	-.175	-.15	-.13					
-1.00	-.22	-.205	-.20	-.195	-.19	-.185	-.17	-.15	-.125					
-0.75	-.205	-.19	-.185	-.18	-.18	-.18	-.165	-.145	-.125					
-0.50	-.185	-.18	-.175	-.175	-.175	-.17	-.16	-.14	-.12	-.09	-.06			
-0.25	-.17	-.17	-.165	-.165	-.16	-.16	-.145	-.13	-.11	-.09	-.065	-.03		
0.0	-.155	-.155	-.15	-.15	-.15	-.14	-.13	-.115	-.105	-.085	-.065	-.035		
0.25	-.135	-.135		-.13	-.13	-.125	-.115	-.105	-.095	-.075	-.06	-.03	+.02	
0.50	-.115				-.115	-.11	-.10	-.09	-.085	-.07	-.05	-.025	+.015	
0.75	-.095					-.095	-.085	-.075	-.07	-.055	-.035	-.01	+.02	
1.00	-.075					-.075	-.07	-.055	-.05	-.035	-.015	+.005	+.03	+.13
1.25						-.05	-.04	-.025	-.025	-.005	+.01	+.03	+.05	+.13
1.50						-.015	.00	+.01	+.01	+.025	+.04	+.055	+.075	+.14
1.75						+.03	+.04	+.05	+.05	+.06	+.07	+.09	+.105	+.165
2.00						+.09	+.09	+.09	+.09	+.10	+.105	+.125	+.15	+.195
2.25						+.145	+.145	+.145	+.145	+.15	+.15		+.19	+.23
2.50						+.20	+.20	+.20	+.20	+.21	+.21		+.24	+.27
2.75							+.26	+.26	+.26	+.26	+.26		+.275	+.315
3.00							+.31	+.31	+.31	+.31	+.31		+.32	+.35
3.25								+.355					+.365	+.39
3.50								+.40					+.40	+.42
3.75								+.44						+.455
4.00								+.475						+.495
4.25								+.51						+.53
4.50								+.56						+.565
4.75								+.60						+.60
5.00								+.65						+.65

been used to build the composite diagrams of each age group. As Mermilliod (1980a) stated, the clusters have been fitted to the chosen representative clusters by using the real sequences instead of idealized ones.

The ZAMS is identical to the sequence drawn for the NGC 6231 age group in the B-type stars domain up to $M_V = -2$ and results from the superimposition of the sequences for A- and F-type stars, down to $M_V = +5$. The values are listed in Table 6. Figs. 4 and 5 show that the new sequences are very similar to Blaauw's (1963) but strongly differ from Eggen's (1976). Clearly the present ZAMS, obtained quite independently, is not in keeping with the revision proposed by Eggen. It is also very close to the ZAMS for Pleiades stars published by Turner (1979). In the range $0.10 < (B-V)_0 < 0.50$, the difference in M_V at constant $(B-V)_0$ is only 0.02 mag.

The cut-off of the ZAMS has been chosen to avoid evolutionary effects. However it cannot be proved that the present ZAMS is strictly unevolved at $M_V = -2$, before working out younger clusters in the same manner. But for O-type stars, the photometric indices in the visual

domain become insensitive to temperature so that the distinction between age groups with turn-up at O-types will be photometrically difficult. It is then expected that the ZAMS will not become much bluer at a given M_V .

The determination of the upper part of the ZAMS ($M_V < -2$) depends critically on the correction of differential reddening which is always present in the youngest clusters embedded in nebulae.

At present, the faint red part of the ZAMS cannot be defined by open clusters only. K and M dwarfs have been observed in the Hyades, but the deduced sequence is valid for stars of the same chemical composition only. Solar chemical composition is thought to be shared by the Pleiades stars, but the K dwarfs of this cluster are affected by the flare phenomenon so that their usefulness for the ZAMS determination is questionable. Main sequence K and M dwarfs have not been observed photoelectrically in any other clusters.

5. Absolute Ageing

Various parameters have been proposed to estimate the clusters' ages, among others by Lindoff (1968) and

Table 4. Normal points in the M_V vs $(U-B)_O$ isochronous curves

M_V	6231	2362	884	457	3766	IC4665	α Per	Plei	2516	2287	6475	3532	2281	Hyades
-4.50	-1.115	-1.04												
-4.25	-1.11	-1.04												
-4.00	-1.105	-1.04	-.95											
-3.75	-1.095	-1.035	-.95	-.88										
-3.50	-1.085	-1.03	-.95	-.88										
-3.25	-1.07	-1.02	-.945	-.88										
-3.00	-1.05	-1.005	-.935	-.875	-.80									
-2.75	-1.035	-0.99	-.92	-.86	-.80									
-2.50	-1.015	-0.97	-.90	-.85	-.795									
-2.25	-0.99	-0.945	-.875	-.835	-.79	-.66	-.59							
-2.00	-0.96	-0.915	-.845	-.815	-.785	-.675	-.59							
-1.75	-.92	-0.875	-.82	-.795	-.77	-.68	-.60							
-1.50	-.875	-.835	-.785	-.77	-.75	-.68	-.60	-.50	-.42					
-1.25	-.825	-.795	-.75	-.74	-.725	-.675	-.60	-.50	-.42					
-1.00	-.775	-.745	-.71	-.70	-.69	-.655	-.595	-.50	-.41					
-0.75	-.71	-.69	-.665	-.66	-.645	-.625	-.575	-.49	-.40					
-0.50	-.64	-.635	-.615	-.61	-.60	-.58	-.54	-.46	-.37	-.24	-.15			
-0.25	-.57	-.57	-.56	-.555	-.545	-.525	-.48	-.42	-.34	-.24	-.165	-.06		
0.0	-.50	-.50	-.495	-.49	-.485	-.46	-.42	-.37	-.30	-.225	-.16	-.07		
0.25	-.43	-.43	-.425	-.42	-.42	-.40	-.365	-.315	-.26	-.185	-.135	-.06	.00	
0.50	-.36	-.36	-.355	-.35	-.35	-.335	-.30	-.24	-.215	-.16	-.105	-.035	.00	
0.75	-.285	-.285	-.28	-.28	-.28	-.265	-.24	-.175	-.16	-.12	-.06	-.015	+.01	
1.00	-.20	-.20	-.20	-.20	-.20	-.185	-.165	-.11	-.10	-.06	-.02	+.005	+.02	+.13
1.25					-.105	-.10	-.085	-.04	-.035	.00	+.02	+.035	+.045	+.13
1.50					-.02	-.02	-.005	+.02	+.02	+.035	+.055	+.06	+.065	+.125
1.75						+.05	+.06	+.06	+.06	+.065	+.075	+.08	+.085	+.12
2.00						+.08	+.085	+.085	+.085	+.085	+.09	+.095	+.10	+.11
2.25							+.095	+.095	+.095	+.095	+.095		+.10	+.095
2.50							+.085	+.085	+.085	+.085	+.085		+.09	+.075
2.75							+.06	+.06			+.06		+.065	+.05
3.00							+.03	+.03			+.03		+.035	+.025
3.25													.00	+.005
3.50													-.01	-.005
3.75														+.005
4.00														+.015
4.25														+.04
4.50														+.075
4.75														+.12
5.00														+.18

Table 5. Intrinsic colour-colour UBV relations

$(U-B)_O$	$(B-V)_O$	$(U-B)_O$	$(B-V)_O$
-1.05	-.30	-.15	-.065
-1.00	-.28	-.10	-.05
-.95	-.265	-.05	-.03
-.90	-.25	.00	.00
-.85	-.235	.02	.025
-.80	-.225	.05	.055
-.75	-.21	.07	.07
-.70	-.20	.10	.085
-.65	-.185	.15	.095
-.60	-.175	.20	.085
-.55	-.165	.25	.065
-.50	-.15	.30	.035
-.45	-.14	.35	.01
-.40	-.125	.40	-.01
-.35	-.115	.45	-.01
-.30	-.105	.50	.00
-.25	-.095	.55	.04
-.20	-.08	.60	.105

Table 6. Normal points of the ZAMS

M_V	$(B-V)_O$	$(U-B)_O$	M_V	$(B-V)_O$	$(U-B)_O$
-2.00	-.265	-.96	1.50	-.015	-.02
-1.75	-.255	-.92	1.75	.03	.035
-1.50	-.245	-.875	2.00	.08	.075
-1.25	-.235	-.825	2.25	.145	.095
-1.00	-.22	-.775	2.50	.20	.085
-0.75	-.205	-.71	2.75	.26	.06
-0.50	-.185	-.64	3.00	.31	.03
-0.25	-.17	-.58	3.25	.355	.01
0.00	-.15	-.50	3.50	.40	-.01
0.25	-.135	-.43	3.75	.44	-.01
0.50	-.115	-.35	4.00	.475	-.01
0.75	-.10	-.28	4.25	.51	.01
1.00	-.08	-.20	4.50	.56	.01
1.25	-.05	-.10	4.75	.60	.10
			5.00	.65	.15

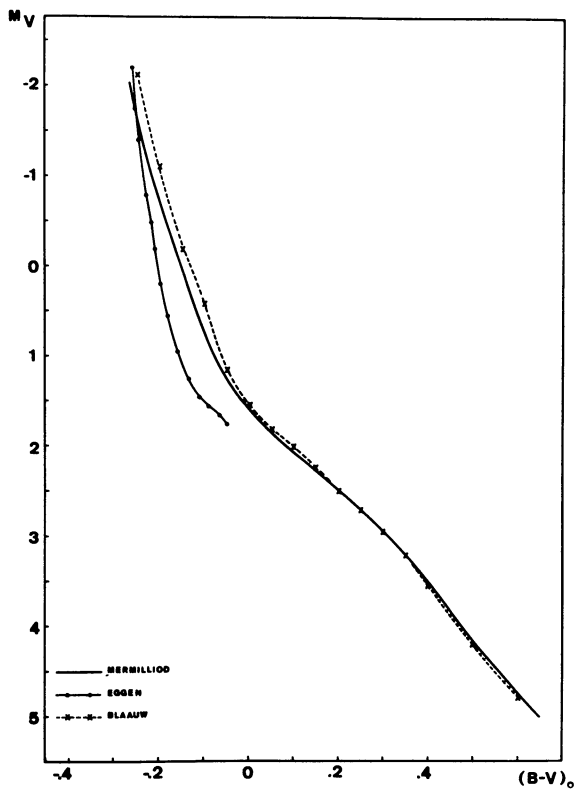


Fig. 4. Comparison of the present ZAMS with Blaauw's (1963) and Eggen's (1976). This sequence does not favour the revision proposed by Eggen.

Harris (1976). The former author devised a parameter Γ which is applicable to clusters throughout the whole age range but the relation Γ vs $\log t$ does not seem to be single-valued for the youngest clusters. The latter used a parameter A_{12} taking into account the two brightest stars and applicable to clusters younger than the Hyades. The signification of A_{12} is not always straightforward, in particular when one of the two stars is a blue straggler, like in NGC 2516 (turn-up type at B8, blue straggler type = B2), since it is formed from the $U-B$ colours and spectral types, which may differ by several tenths or subclasses respectively.

From examination of the composite diagrams and especially from Fig. 2, it appears that the best age parameter is the bluest point on the mean main sequence of the clusters. Such a criterion has already been applied by Stothers (1972) (point "e" on his curve, Fig. 1). This point is rather easy to determine experimentally since the evolved sequence is nearly vertical and binarity effects are less pronounced. A calibration of this parameter versus $\log t$ has been obtained from Maeder's new grid of models with overshooting in the core (Maeder and Mermilliod, 1981) by the following procedure.

M_{bol} and $\log T_{eff}$ values have been transformed into M_V and $(B-V)_0$ respectively using Flower's (1977) tables, and from $(B-V)_0$ into $(U-B)_0$ according to Heintze (1973). The relation between $\log t$ and the theoretical bluest $(U-B)_0$ point on the isochrones has been drawn (Fig. 6). The calibration can be divided into two parts so that a linear relation holds for each one separately:

$$\begin{aligned} -0.80 \leq (U-B)_0 < -0.35 \quad \log t &= 1.795(U-B)_0 + 8.785 & (a) \\ -0.28 \leq (U-B)_0 < 0.00 \quad \log t &= 0.813(U-B)_0 + 8.487 & (b) \end{aligned}$$

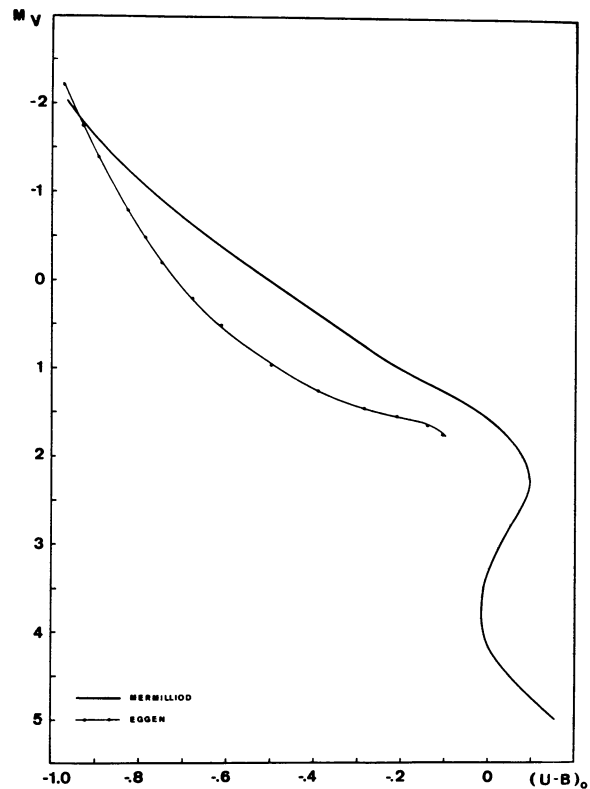


Fig. 5. Comparison of the ZAMS (present work) and Eggen's (1976) sequence.

Thus, the age is slightly overestimated in the curved portion of the relation if one uses these linear equations for $-0.35 < (U-B)_0 < -0.28$.

Table 7 contains the parameters of each age group:

- 1) the name of the representative cluster,
- 2) the list of clusters included in each age group,
- 3) the bluest $(B-V)_0$ and $(U-B)_0$ colour indices, estimated from the present sequences,
- 4) the earliest spectral type on the main sequence as obtained from the presently available MK classification. For the age groups 1 to 9 the recent works of Abt and Levato, summarized in Abt (1979), have been used. Equivalent types estimated from the bluest colour indices are also given.
- 5) Absolute ages, expressed both in terms of $\log t$ and t , resulting from the calibration described above, are given in the last two columns. No data have been indicated for the youngest groups since the grid of models is not yet completed.

Table 7 shows that the parameter formed with the bluest $(B-V)_0$ colour index varies from 0.13 to -0.32, i.e. over a range of 0.45 mag, whereas the one formed with the $(U-B)_0$ colour index varies from 0.13 to -1.11, or 1.24 mag. This comparison shows the greater potential value of the bluest $(U-B)_0$ parameter as an age discriminator, in spite of the observational difficulties often referred to. This parameter may be more difficult to estimate for an individual cluster, especially when handling a poor one, but one can interpolate the cluster sequence between the present ones.

One also notices in Table 7 that a correspondence can be established between the spectral MK types and age groups over the whole interval from O9 to A2. It

Table 7. Age group parameters

Group	Contents	$(B-V)_0$	$(U-B)_0$	MK	S.T. phot.	log t	age
(1) Hyades	Praesepe, NGC 2539, 6633	.13	.13	A2	-	8.82	$6.61 \cdot 10^8$
(2) NGC 2281	NGC 1342, 1662, 1664, 2251, 2548, 2437, 2099 7209	.015	.00	A1	A0.5	8.48	$3.02 \cdot 10^8$
(3) NGC 3532	NGC 7092, 1528	-.035	-.07	B9.5-A0	B9.7	8.43	$2.69 \cdot 10^8$
(4) NGC 6475	NGC 6281, 1912, 4349, 6259, 6281, 6494, 6705	-.065	-.165	B9	B9.2	8.35	$2.24 \cdot 10^8$
(5) NGC 2287	NGC 1039, 5316	-.09	-.24	B8.5-B9	B8.7	8.29	$1.95 \cdot 10^8$
(6) NGC 2516	NGC 2168, 2301, 3114, 5460, 6025:, 7243	-.13	-.42	B8.5	B7.0	8.03	$1.07 \cdot 10^8$
(7) Pleiades	NGC 2323, 2422, 6067, 6709, 7790, Tr 2	-.15	-.50	B6	B6	7.89	$7.76 \cdot 10^7$
(8) α Per	5281, 6242, 6405	-.175	-.60	B5	B4.8	7.71	$5.13 \cdot 10^7$
(9) IC 4665	NGC 2451, 4609 IC 2391, IC 2602	-.195	-.68	B3	B3.5	7.56	$3.63 \cdot 10^7$
(10) NGC 3766	NGC 581, 663, 2232 2571, 4103, Cr 140	-.215	-.80	B2	B2.5	7.35	$2.24 \cdot 10^7$
(11) NGC 457	NGC 654, 957, 1960, 2439 3590	-.23	-.88	B1	B2		
(12) NGC 884	NGC 4755, 6871, IC 2581	-.24	-.95	B0.5	B1		
(13) NGC 2362	NGC 1502, 2169, 6531, 7160	-.27	-1.04	B0	B0.5		
(14) NGC 6231	NGC 2264, Orion cluster	-.32	-1.11	O9	O9.5		

is concluded that the bluest spectral type (excluding blue stragglers) is a good primary age indicator. The estimation is better from O9 to B6 because the relation between spectral type and colours is narrower. On the other hand, between B8 and A0, the efficiency of the age discrimination is lower because the mean distance along the $U-B$ axis is greater from one subclass to the other.

The groups have been treated as a whole and no attempt has been made to date the clusters individually. More photoelectric data than presently available would be necessary to draw more complete diagrams, resulting in a better definition of the sequences. The ages obtained are mainly those of the clusters which define the age groups, since they play a great part in the definition of the observed sequences.

The apparent age dispersion within a group depends, on the one hand, on the systematic errors in the photometry. It is hoped that they have been correctly taken into account by inter-comparison of the available sets of data (Mermilliod, 1980b), and they should be equal to or smaller than 0.02 on the $U-B$ index. On the other hand, it depends also on other causes that may introduce changes in the energy distribution of the stars, as discussed below.

Effects due to difference in chemical composition are not expected to play a significant role, since the clusters are young and, in majority, closer than 1 kpc, thus leading to a small dispersion in chemical composition. (This is, however, not true for NGC 6705 (M11),

whose red giants are redder in $B-V$ than other red giants of similar age). Moreover, the UBV colour indices for B-type stars are not sensitive to chemical composition.

Effects of the rotational reddening for stars with large $v \sin i$ have not been corrected. Because of the lack of $v \sin i$ data for a very large fraction of the clusters, it has been assumed that the $v \sin i$ distribution in clusters of similar age and stellar content is roughly the same, so that the superimposition of the colour-magnitude diagrams does not result in too great an age scatter. It is also assumed that there exists a significant fraction of moderately rotating stars whose colours are not influenced by rotation, and which can be used to determine the empirical isochronous curves.

The true age dispersion within a group depends on the real scatter of the ages of the clusters. It has been estimated by measuring the mean distances along the $U-B$ axis of the "single" stars in a given cluster to the M_V , $(U-B)_0$ isochronous curve of its group. The maximum value of the difference between the age of a cluster and the mean age of the group to which it belongs amounts to 0.05 in log t for the younger clusters (part "a" of the age calibration) and to 0.02 in log t for the older (part "b"). From the data contained in Table 7, the smaller difference in log t between two consecutive age groups is 0.14-0.15 for the younger groups ($(U-B)_0 < -.35$) and 0.05-0.06 for the older ($(U-B)_0 > -.28$). The age scatter within a group thus represents one-third of the smaller age interval between two consecutive groups.

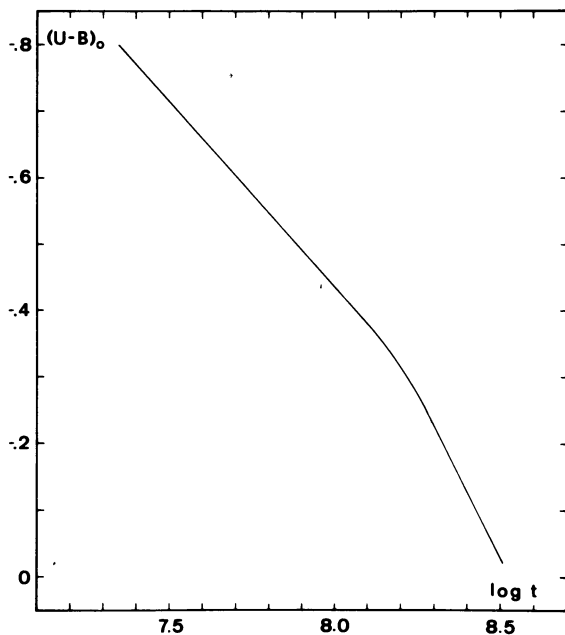


Fig. 6. Calibration of the bluest $(U-B)_0$ on the main sequence in terms of age ($\log t$)

6. Discussion

The synthetic composite diagram presented in Fig. 1 contains a lot of information about stellar evolution and some aspects will be discussed here.

Evolution on the main sequence for single stars is rather well understood. The present models, and especially those with overshooting in the core (Maeder and Mermilliod, 1981) reproduce the observed patterns quite correctly. As said before, the exact termination of the main sequence is difficult to determine experimentally and has been adopted from the models.

But there are fewer theoretical predictions on the red giants' position in the HR diagram of young open clusters and this section will be devoted mainly to the examination of the red evolved stars according to the composite diagrams' features (Fig. 1 and those in Mermilliod (1980a)). From these diagrams, it is evident that very few stars are located in the middle of the Hertzsprung gap. Those found are either Cepheids or composite spectroscopic binaries (gK + dA). A few highly evolved very luminous supergiants are also found in the youngest groups. This fact imposes some constraints on the models describing loops in the HR diagram.

One notices also that the red giants do not form a "branch", but are rather grouped, and that two distinct trends in the patterns of red giant concentrations are noticeable. In the first four age groups (the Hyades to NGC 6475), their mean positions remain at a fixed $(B-V)_0$, equal to +1.0, while the absolute magnitude becomes brighter. This fact is to be compared to the position of the clump of red giants in older open clusters at $M_V=+1$ and $(B-V)_0=+1.0$ (Grenon, 1978), independently of their ages. Faulkner and Cannon (1973) demonstrated from evolutionary models that these stars are in the helium core-burning phase. From the observed fixed position of the red giant concentra-

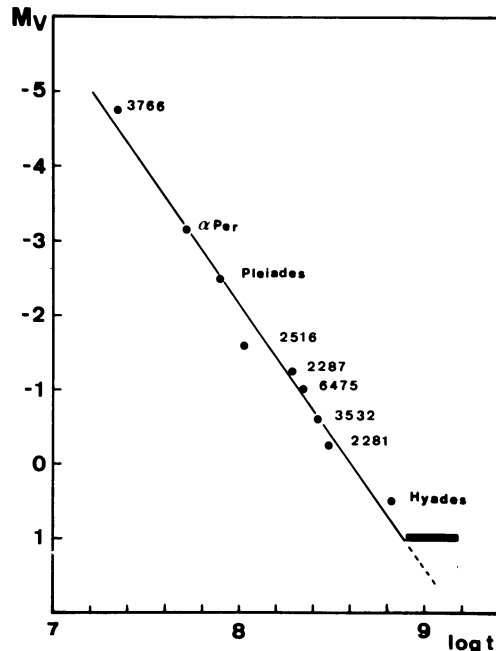


Fig. 7. Relation between the mean absolute magnitude of the red giant concentrations and $\log t$. The darkened area at $M_V=+1$ indicates the position of the clump in old clusters.

tions in these four younger age groups, we may infer that most of the red giants are also in the helium core-burning phase, which leads to the observation of a well-defined clump.

One notices in the composite diagrams (Mermilliod, 1980a) that the concentration is better marked in these groups (especially at the Hyades age, due to better precision in the photometric data) than in the younger ones. These features have been foreseen by Cannon (1970).

From the NGC 2287 age group on, the $(B-V)_0$ colour index of the concentration is redder and redder as the absolute magnitude becomes brighter, and the luminosity classes change gradually (see Keenan, 1973).

Table 8 gives the position of the giants' concentrations schematized in Fig. 1. It contains the age group name, the mean absolute magnitude M_V and mean colour index $(B-V)_0$, the most frequent spectral type and corresponding M_{bol} and $\log T_{eff}$ calculated from the M_V and $(B-V)_0$ values using Flower's (1975) transformation, and $\log t$ (from Table 7).

A correlation has been established between the mean absolute magnitude of the red giant concentrations and ages (Fig. 7). A straight line has been fitted by eye, which gives the following relation:

$$\log t = 0.280 M_V + 8.610$$

This relation offers the opportunity of estimating the age of an open cluster if it presents a sufficiently well marked giant concentration. Evidently, this possibility holds for the age range under consideration and should not be applied to older clusters in which the absolute magnitude of the clump is constant. From Fig. 7 one sees that this turns out to be the case for clusters older than 8.9 in $\log t$.

Table 8. Mean positions of the giants' concentrations

Groups	M_V	$(B-V)_0$	T.S.	M_{bol}	$\log T_{eff}$	$\log t$
Hyades	+0.5	.98	G8-K0III	+0.2	3.686	8.82
NGC 2281	-0.25	1.00	G8-K0III	-0.6	3.682	8.48
3532	-0.60	.95	G8-K0III	-0.95	3.692	8.43
6475	-1.0	1.03	(K0III)	-1.4	3.676	8.35
2287	-1.25	1.07	K0II-III	-1.65	3.668	8.29
2516	-1.6	1.13	(K1II)	-2.06	3.656	8.03
Pleiades	-2.5	1.25	K2-3II	-3.1	3.632	7.89
α Per	-3.15	1.47	K2II-Ib	-3.9	3.602	7.71
IC 4665	(-2.9)	1.7	(K5Ia)	-	-	7.56
NGC 3766	-4.75	1.70	M0Ib	-5.2	3.544	7.35
457	-5.4	1.8	M2Ib	-8.8	3.447	
884	-5.5	1.8	M0-M2Iab	-8.9	3.447	
2362	-	-	-	-	-	-
6231	-	-	-	-	-	-

At this point it may be useful to recall that the properties of the red giants not only rely on the photometric analysis, but primarily rest on the results of an extensive programme of photoelectric radial velocities for all red giants in clusters north of -20° , down to $B=12.5$ (Mermilliod and Mayor, 1980). The photometric analysis of the southern clusters ($\delta < -20^\circ$) has been adapted to the results obtained for the northern ones according to the radial velocity membership.

As can be seen in Fig. 1, the Cepheid variables are somewhat grouped in a small area in the middle of the Hertzsprung gap. In fact, the values of the periods of the 11 Cepheids presently associated with open clusters are between 3 and 11 days. Statistics based on 184 stars nearer to the Sun than 3 kpc extracted from the catalogue of Fernie and Hube (1968) show that 80% of the Cepheids fall in this periods interval (Fig. 8). Thus the bulk of the Cepheids have ages corresponding to open clusters with spectral type at turn-up between B4/5 and B8, i.e. $5 \times 10^7 < t < 10 \times 10^7$.

The M supergiants occupy also a small zone in Fig. 1. This is partly because the $B-V$ index becomes insensitive to temperature at these types. However, the spectral types are fairly grouped around those indicated in Table 7. The occurrence of this kind of star is age-limited and presents a threshold. The present investigation confirms the finding of Schild (1970) who showed that red supergiants are not associated with clusters with turn-up earlier or equal to B0. However, the sample of investigated clusters is still very small, including several poor star clusters, so that a definitive conclusion on the absence of red supergiants in very young open clusters with turn-up at B0 may await confirmation. Further examination of young clusters like Tr 37 (Garrison and Kormendy, 1976) (turn-up at 09.5-B0) should prove interesting if the red supergiant μ Cep (M2Ia) is really a member, or like Tr 27 (Moffat et al., 1977) (turn-up approximately at the same type, although less well defined) which contains an M0Ia supergiant very near the cluster centre.

7. Conclusion

A complete set of empirical isochronous curves for 14 age groups of open clusters younger than the Hyades has been presented. This led to the redetermination of the

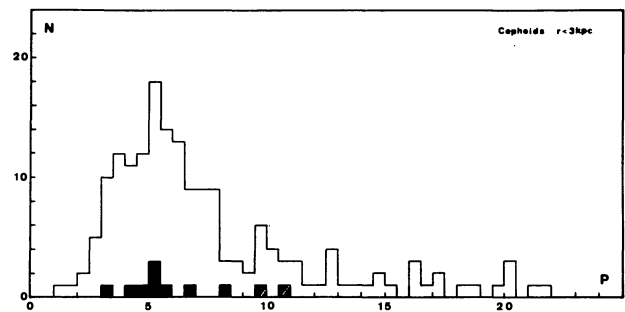


Fig. 8. Distribution of the periods of the galactic Cepheids nearer to the Sun than 3 kpc. The hatched zone corresponds to the Cepheids members of open clusters. 80% of the periods are smaller than 11 days.

$U-B/B-V$ relation and of the ZAMS. The latter appears to confirm the sequence of Blaauw (1963) and to conflict seriously with the revised ZAMS proposed by Eggen (1976).

The synthetic composite HR diagram built resulted in obtaining information connected to stellar evolution in the red giant region.

The new classification scheme of young open clusters by means of age groups can be used to tackle a wide variety of problems and furnishes a new scenario to compare open clusters among each other.

The absolute age calibration will permit dating of young open clusters on the same scale, replacing the diversity of calibration presently available. Expedient methods like those used in the past to determine ages should be left out and replaced by one which is more precise: all the information contained in the HR diagram ought to be used, and not only that obtained from a few brightest stars.

Much more data are needed to refine the picture that has been drawn, and the possibilities of the classification scheme will be improved when better photometric and more numerous spectroscopic data become available. A complete MK classification of the red giants according to the fine luminosity subclasses devised by Keenan (1973) would be very useful.

References

- Abt H.A.: 1979, *Astrophys. J.* 230, 485.
- Barbaro G., Dallaporta N., Fabris G.: 1968, in *Mass Loss from Stars*, Ed. M. Hack, Trieste, p. 89.
- Blaauw A.: 1963, in *Basic Astronomical Data*, Ed. K.A. Strand, p. 383.
- Böhm-Vitense E., Canterna R.: 1974, *Astrophys. J.* 194, 629.
- Cannon R.D.: 1970, *Mon. Not. R. Astr. Soc.* 150, 111.
- Deutschman W.A., Davis R.J., Schild R.E.: 1976, *Astrophys. J. Suppl.* 30, 97.
- Eggen O.J.: 1976, *Quart. J. R. Astr. Soc.* 17, 472.
- Faulkner D.J., Cannon R.D.: 1973, *Astrophys. J.* 180, 435.
- Fernie J.D., Hube J.O.: 1968, *Astron. J.* 73, 492.
- Flower P.J.: 1975, *Astron. Astrophys.* 41, 391.
- Flower P.J.: 1977, *Astron. Astrophys.* 54, 31.
- Garrison R.J., Kormendy J.: 1976, *Publ. Astron. Soc. Pacific* 88, 865.

- Golay M.: 1974, *Introduction to Astronomical Photometry*, Ed. Reidel, p. 79-80.
- Grenon M.: 1978, *Publ. Obs. Geneva Ser. B fasc. 5*.
- Gutierrez-Moreno A.: 1974, *Publ. Astron. Soc. Pacific* 91, 642.
- Harris G.L.H.: 1976, *Astron. J. Suppl.* 30, 451.
- Heintze J.R.W.: 1973, in *IAU Symp. no. 54*, Ed. B. Hauck and B.E. Westerlund (Reidel), p. 231.
- Keenan Ph.: 1973, in *IAU Symp. no. 54*, Ed. B. Hauck and B.E. Westerlund (Reidel), p. 68.
- Maeder A., Mermilliod J.-C.: 1981, *Astron. Astrophys.* 93, 136.
- Mermilliod J.-C.: 1976, *Astron. Astrophys. Suppl.* 24, 159.
- Mermilliod J.-C.: 1980, in *Star Clusters, IAU Symp. no. 85*, Ed. J.E. Hesser (Reidel), p. 129.
- Mermilliod J.-C.: 1980a, *Astron. Astrophys. Suppl.* (submitted for publication) (paper II).
- Mermilliod J.-C.: 1980b, Thesis (Geneva).
- Mermilliod J.-C., Mayor M.: 1980, in *Star Clusters, IAU Symp. no. 85*, Ed. J.E. Hesser (Reidel), p. 361.
- Moffat A.F.J., Fitzgerald M.P., Jackson P.D.: 1977, *Astrophys. J.* 215, 106.
- Sandage A.: 1957, *Astrophys. J.* 125, 436.
- Sandage A., Tamman G.A., *Astrophys. J.* 157, 683.
- Schild R.E.: 1970, *Astrophys. J.* 161, 855.
- Stothers R.: 1972, *Astrophys. J.* 175, 431.
- Turner D.G.: 1978, *J. Roy. Astron. Soc. Can.* 72, 248.
- Turner D.G.: 1979, *Publ. Astron. Soc. Pacific* 91, 642.